Journal of Chromatography, 346 (1985) 1–15
Elsevier Science Publishers B.V., Amsterdam — Printed in The Netherlands

CHROM. 17 959

THEORY OF ANION CONTRIBUTIONS TO NON-LINEAR ELECTRON-CAPTURE DETECTOR RESPONSE

GREGORY WELLS
Varian Instrument Group, Walnut Creek Division, 2700 Mitchell Drive, Walnut Creek, CA 94598 (U.S.A.)
(Received June 10th, 1985)

SUMMARY

A theoretical model is developed to investigate the effects of anion collection on the linear response of the constant-current mode of operation of an electron-capture detector. The results indicate that a non-linear response is expected at high pulse frequencies. The dependence of the linear range on reference current, base frequency, electron concentration and attachment rate constant is examined. A means of extending the linear range by preventing the collection of anions is discussed.

INTRODUCTION

Many theories have been formulated to describe the basic operation of electron-capture detectors. The earliest kinetic model was that of Wentworth *et al.*[1] for the constant-frequency pulsed mode of operation. This mode suffers from having a limited linear range. A substantial improvement in the linear response was effected by Maggs *et al.*[2] who suggested that the electron-capture detector be operated in the constant-current mode. Using a simplified form of Wentworth's equation, in which the reverse of the electron attachment process was neglected, Maggs showed that the collected current I, for a given electron production rate per unit volume $k_p q$, in a cell of volume V, is given by

$$I = \frac{k_p q V}{(k_d + ck_1)T}\left[1 - e^{-(k_d + ck_1)T}\right] \quad (1)$$

where c is the sample concentration, k_1 the attachment rate constant, k_d the pseudo recombination rate constant and T is the pulse period. If the pulse frequency ($f = 1/T$) is changed as the sample concentration is varied, so as to keep the collected current I equal to a constant reference current I, then

$$(k_d + ck_1)\,T = K = (k_d + ck_1)/f \quad (2)$$

0021-9673/85/$03.30

where K is a constant. The change in frequency is proportional to the sample concentration and is given by

$$f - f_0 = c\frac{k_1}{K} \tag{3}$$

where $f_0 = k_d/K$ ($c = 0$).

Although the constant-current mode was found to significantly increase the linear range of the electron-capture detector, the linearity was not limitless as is implied by eqns. 1–3. Some additional mechanisms must exist to account for the observed non-linear response at high sample concentrations. The inability of this model to account for this discrepancy is due to the simplifying assumptions that were made in deriving these equations. An extended analysis by Sliwka *et al.*[3] included the effects of the finite pulse width and electron drift velocity in the operation of the electron-capture detector. More recently Gobby *et al.*[4] investigated many of the assumptions of these theories and proposed a model based on space charge driven charge migration, which included the dynamical effects of the positive ions. Although many of the basic assumptions were quite different from those of the classical model, the resulting equations describing the response as a function of sample concentration were identical to those derived by Wentworth. These models were quite successful in describing most of the main features that have been experimentally observed for small sample concentrations. Lovelock[5,6], and Knighton and Grimsrud[7,8] have successfully applied similar theories to the case of strongly attaching compounds, where the effective concentration of analyte in the detector cell is reduced due to destructive electron attachment. However, none of the models even qualitatively can account for the loss in detector sensitivity that is known to occur at higher sample concentrations for the constant-current electron-capture detector.

In this paper a theoretical model which includes the collection of anions is used to investigate the importance of this process in the reduction of the response. It will be shown that many of the experimentally observed features that occur at large sample concentrations can be qualitatively explained in terms of anion collection effects.

MATHEMATICAL MODEL

The analysis presented here not only includes those processes involving the electrons, but also specifically takes into account the dynamic effects of the anions formed by the electron-attachment process. The chemical processes to be considered are listed in eqns. 4a–4d and are: (4a) ^{63}Ni-induced thermal electron formation; (4b) irreversible electron attachment; (4c) loss of electrons by recombination with positive ions; and (4d) loss of anions by recombination with positive ions. In addition to the chemical processes the dynamic effect of charge removal by the applied electric field must be included. These processes are given in eqn. 5.

$$P + \beta^* \xrightarrow{k_p} P^+ + e^- + \beta \tag{4a}$$

$$A + e^- \xrightarrow{k_1} A^- \tag{4b}$$

$$P^+ + e^- \xrightarrow{k_{2e}} N' \tag{4c}$$

$$P^+ + A^- \xrightarrow{k_{2A}} N'' \tag{4d}$$

$$c^- \xrightarrow{k_{3e}} \text{Anode} \tag{5a}$$

$$A^- \xrightarrow{k_{3A}} \text{Anode} \tag{5b}$$

The rate equations to be solved that describe the processes given in eqns. 4 and 5 can be divided into two different time regions. Region A where the electric field is on ($0 \leqslant t \leqslant t_p$), where t_p is pulse width; and region B where the electric field is off ($t_p \leqslant t \leqslant T$), where T is the pulse period. The differential equations for the two regions are given in eqns. 6 and 7.

(A) $0 \leqslant t \leqslant t_p$

$$\frac{d(e^-)}{dt} = k_p - k_e(e^-) \tag{6a}$$

$$\frac{d(A^-)}{dt} = k_1(A)(e^-) - k_A(A^-) \tag{6b}$$

$$k_e = k_1(A) + (P^+)k_{2e} + k_{3e} \tag{6c}$$

$$k_A = k_{2A}(P^+) + k_{3A} \tag{6d}$$

(B) $t_p < t \leqslant T$

$$\frac{d(e^-)}{dt} = k_p - k'_e(e^-) \tag{7a}$$

$$\frac{d(A^-)}{dt} = k_1(A)(e^-) - k'_A(A^-) \tag{7b}$$

$$k'_e = k_1(A) + (P^+)k_{2e} \tag{7c}$$

$$k'_A = k_{2A}(P^+) \tag{7d}$$

In order to make analytical solutions to eqns. 6 and 7 more tractable, some assumptions need to be made. The first assumption is that the processes within the cell are homogeneous. Grimsrud and Connally[9] have investigated the spacial distribution of ions and electrons within cells of cylindrical symmetry. He has found that for a cell with a diameter of 5 mm, the relative ion density at the center is only 20% less than

at the walls where the ^{63}Ni source is located. This is sufficiently homogeneous for the discussion given here. The rate at which electrons and positive ions are created per unit time and volume can thus be approximated by a constant, k_p. The second assumption is that the positive ion density remains constant, independent of pulse frequency. This would allow the quantities involving (P^+) in eqns. 6c and d, and 7c and d to be taken as constants. The results of Gobby *et al.*[4] and the investigations of Grimsrud and co-workers[8,10–12] indicate that this is a quite reasonable assumption for the constant current mode of operation. The last approximation is that the electric field is constant throughout the cell. This allows the rate constant for charge removal by the field to be expressed as a constant

$$k_{3e} = v_e A/V \tag{8a}$$

$$k_{3A} = v_A A/V \tag{8b}$$

$$v_{e,A} = K_{e,A} U \tag{8c}$$

where $v_{e,A}$ = electron or anion drift velocity; A = area of anode; V = volume of cell; K_e = electron mobility[13,14]; K_A = anion mobility[13,14]; U = cell potential.

Although these rate constants are strictly true only for constant electric fields, E (*i.e.*, parallel planar electrode geometry where $E \propto U$) this approximation should be reasonable if the average field is used and since all other kinetic processes have been assumed to be homogeneous throughout the cell. A more detailed analysis of this assumption will be made in a later section of this paper.

It can be seen from eqns. 6b and 7b that the solutions of the equations for the anions require a knowledge of the electron concentrations as a function of time for the time intervals A and B. The solution of eqn. 6a for region A for one time cycle is

$$(e^-)_t = \frac{k_p}{k_e} + \left[(e^-)_0 - \frac{k_p}{k_e}\right] e^{-k_e t} \tag{9}$$

where $(e^-)_0$ is the electron concentration at $t = 0$, which is initially unknown, but must match that at the end of the first time cycle $t = T$. The general solution of eqn. 7a for region B is

$$(e^-)_t = \frac{k_p}{k'_e} + \left[(e^-)_{t_p} - \frac{k_p}{k'_e}\right] e^{-k'_e (t - t_p)} \tag{10}$$

The solution given in eqn. 10 for $t = T$ can be used to solve for $(e^-)_t$ in region A for the next cycle of time. The electron concentration after m cycles at the beginning of the voltage pulse in region A at time mT is

$$(e^-)_{mT} = \frac{k_p}{k'_e} + \left[(e^-)_{mt_p} - \frac{k_p}{k'_e}\right] e^{-k'_e (T - t_p)} \tag{11}$$

where

$$(e^-)_{mt_p} = \frac{k_p}{k_e} + \left[(e^-)_{(m-1)T} - \frac{k_p}{k_e}\right] e^{-k_e t_p} \tag{12}$$

After several cycles

$$\lim_{m \to \infty} (e^-)_{mT} = (e^-)_{(m-1)T} \equiv (e^-)_T$$

and

$$\lim_{m \to \infty} (e^-)_{mt_p} = (e^-)_{(m-1)t_p} \equiv (e^-)_{t_p}$$

Thus

$$(e^-)_T = \frac{k_p}{k'_e} + \left\{\frac{k_p}{k_e} + \left[(e^-)_T - \frac{k_p}{k_e}\right] e^{-k' t_p} - \frac{k_p}{k'_e}\right\} e^{-k'_e (T - t_p)} \tag{13}$$

Which allows the electron concentration at the beginning of the extraction pulse in region A to be found

$$(e^-)_T = \frac{\dfrac{k_p}{k'_e} + \left(\dfrac{k_p}{k_e} - \dfrac{k_p}{k'_e}\right) e^{-k'_e(T - t_p)} - \dfrac{k_p}{k'_e} e^{-k_e t_p - k'_e(T - t_p)}}{1 - e^{-k_e t_p - k'_e(T - t_p)}} \tag{14}$$

Thus the general solution of equation 6a for region A is

$$(e^-)_t = \frac{k_p}{k_e} + \left[(e^-)_T - \frac{k_p}{k_e}\right] e^{-k_e t} \tag{15}$$

The electron current collected at the anode during the extraction pulse is

$$I_e = \frac{1}{T} \int_0^{t_p} (e^-)_t \, qAv_e dt \tag{16}$$

where $(e^-)_t$ is given by eqn. 15. The result is

$$I_e = qAv_e \left\{\frac{k_p}{k_e} \frac{t_p}{T} + \frac{k_p}{k_e T} [\chi] \left[1 - e^{-k_e t_p}\right]\right\} \tag{17}$$

$$\chi = \frac{1}{k'_e} + \left(\frac{1}{k_e} - \frac{1}{k'_e}\right) e^{-k'_e(T - t_p)} - \frac{1}{k_e} e^{-k_e t_p - k'_e(T - t_p)} \tag{18}$$

Now that expressions for the electron concentration as a function of time for region A have been obtained, eqn. 15; and for region B, eqn. 10; it is possible to return to eqns. 6b and 7b and solve for the anion concentrations as a function of time. Using the same approach as above and requiring:

$$\lim_{m \to \infty} (A^-)_{mT} = (A^-)_{(m-1)T} \equiv (A^-)_T$$

and

$$\lim_{m \to \infty} (A^-)_{mt_p} = (A^-)_{(m-1)t_p} \equiv (A^-)_{t_p}$$

The resulting solutions are

Region A

$$(A^-)_t = \left[(A^-)_T - \frac{A}{k_A} + \frac{B}{(k_e - k_A)}\right] e^{-k_A t} + \frac{A}{k_A} - \frac{B}{(k_e - k_A)} e^{-k_e t} \tag{19}$$

where

$$A = \frac{k_p k_1}{k_e} \text{ and } B = \left[(e^-)_T - \frac{k_p}{k_e}\right] k_1$$

Region B, $t = T$

$$(A^-)_T = \frac{\left[\frac{-A}{k_A} + \frac{B}{(k_e - k_A)}\right] e^{-k_A t_p} + \frac{A}{k_A} - \frac{B}{(k_e - k_A)} e^{-k_e t_p}}{e^{-k'_A(T - t_p)} - e^{-k_A t_p}} \cdot$$

$$\cdot \frac{\frac{-\alpha}{k'_A} + \frac{\beta}{(k'_e - k'_A)} e^{-k'_e t_p} + \left[\frac{\alpha}{k'_A} - \frac{\beta}{(k'_e - k'_A)} e^{-k'_e T}\right] e^{k'_A(T - t_p)}}{e^{-k'_A(T - t_p)} - e^{-k_A t_p}} \tag{20}$$

where

$$\alpha = \frac{k_p k_1}{k'_e} \text{ and } \beta = k_1 \left\{\frac{k_p}{k_e} + \left[(e^-)_T - \frac{k_p}{k_e}\right] e^{-k_p t_e} - \frac{k_p}{k'_e}\right\} e^{k'_e t_p}$$

The anion contribution to the collected current is thus

$$I_A = \frac{1}{T}\int_0^{t_p} (A^-)_t \, qAv_A dt \tag{21}$$

$$I_A = \frac{qAv_A}{T}\left\{\frac{-1}{k_A}\left[(A^-)_T - \frac{A}{k_A} + \frac{B}{(k_e - k_A)}\right]\left[e^{-k_A t_p} - 1\right] + \right. \tag{22}$$

$$\left. + \frac{A}{k_A} t_p + \frac{B}{k_e(k_e - k_A)}\left[e^{-k_e t_p} - 1\right]\right\}$$

The total current collected at the anode is therefore

$$I_t = I_e + I_A \tag{23}$$

It is of interest to examine some of the limits of each term in eqn. 23. In particular:

$$\lim_{\substack{T \to \text{large} \\ v_A \to \text{small}}} (I_e + I_A) = I_e \tag{24}$$

$$\lim_{t_p/T \to 0} I_e = \left[\frac{qAv_e k_p}{Tk_e}\right]\left[\frac{1}{k'_e} - \frac{1}{k_e}\right]\left[1 - e^{-k'_e T}\right] \tag{25}$$

Using eqns. 6c and 7c to express eqn. 25 explicitly

$$M = \left[\frac{qk_p}{T}\right]\left[\frac{Av_e}{k_1(\chi) + (P^+)\,k_{2e} + \dfrac{v_e A}{V}}\right]\cdot\left[\frac{1}{k_1(\chi) + (P^+)k_{2e}} - \right. \tag{26}$$

$$\left. \frac{1}{k_1(\chi) + (P^+)\,k_{2e} + \dfrac{v_e A}{V}}\right]\left[1 - e^{-(k_1(\chi) + (P^+)\,k_{2e})T}\right]$$

$$\lim_{EK_e \to \text{large}} M = \frac{qk_{pV}}{k'_e}\left[1 - e^{-k'_e T}\right] \tag{27}$$

This is identical to the classical equation of Wentworth, eqn. 1.

EXPERIMENTAL

A Varian Vista 6000 gas chromatograph with a 1075 split/splitless injector was used for this study. A Varian 402 chromatography data system was used to store raw data and process it. The electron-capture detector cell was a standard 0.300 ml displaced coaxial design[15,16] and the constant-current electronics were modified to allow the reference current and pulse voltage to be variable. The detector temperature was maintained at 300°C and 30 ml/min of nitrogen was added to the cell in addition to the 1 ml/min helium column flow. The column was a 15 m × 0.32 mm I.D. bonded methylsilicone (SGE). The calculations for the numerical model were done with a HP1000 computer.

DISCUSSION

Fig. 1 shows a plot of the solution of eqn. 23 for the constant current mode using the parameters listed in Table I, in which the value of the frequency, $f = 1/T$, was iterated until $I_t = I_{ref.}$. The line marked (W) is the solution for the classical Wentworth equation, eqn. 27. The remaining curves are for different values of anion drift velocities; 0–300 cm/sec. In the limit in which the anion drift velocity is equal to that of the electron, they both would contribute equally to the collected current.

Fig. 2 shows sensitivity plots for several compounds. Although each compound has a different sensitivity and hence a different detection limit, the concentration at which the compound sensitivity is decreased by 10% is also different. The result is that the linear range is approximately the same for all of these compounds. In addition, the pulse frequence at which this non-linearity begins is almost the same for every compound, 65 kHz (dashed line in Fig. 2). The only significant property that is different for each compound is the attachment rate constant k_1. From eqns. 6 and 7 it can be seen that this always enters the equations as the product $k_1(A)$. Therefore,

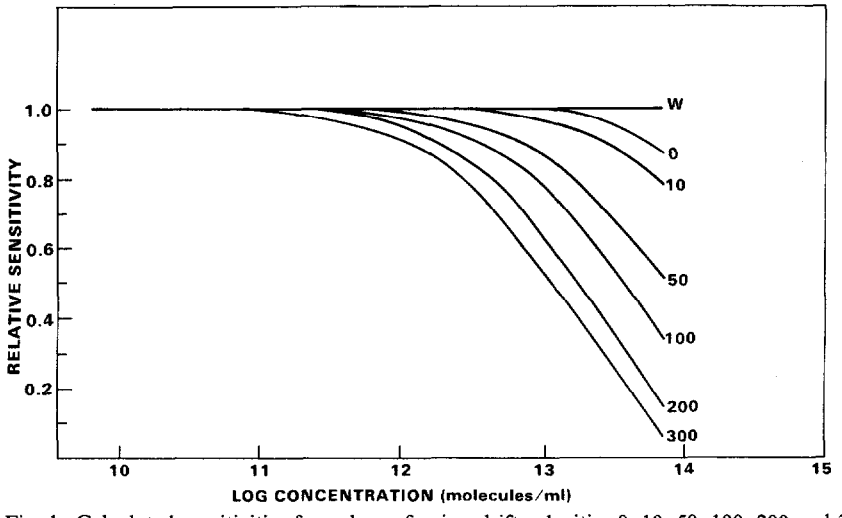

Fig. 1. Calculated sensitivities for values of anion drift velocities 0, 10, 50, 100, 200 and 300 cm/sec.

TABLE I

PARAMETERS FOR CALCULATION

Parameter	*Value*	*Reference Nos.*
k_p	$7.4 \cdot 10^{10}$ ml sec^{-1}	7–12
k_{2e}	$3 \cdot 10^{-6}$ ml sec^{-1}	7–12
k_{2A}	$3 \cdot 10^{-6}$ ml sec^{-1}	7–12
k_1 (lindane)	$8 \cdot 10^{-8}$ ml sec^{-1}	25, 26
(P^+)	$1.6 \cdot 10^{8}$ ml sec^{-1}	7–12
v_e	$3 \cdot 10^{5}$ cm sec^{-1}	21, 22, 24
v_A	200 cm sec^{-1}	23, 24
	40 V	
V	0.300 ml	
A	0.200 cm^2	
t_p	$6 \cdot 10^{-7}$	
I_{ref}	$2.96 \cdot 10^{-10}$ A	
Contaminant concentration (C)	$1 \cdot 10^{10}$ molecules ml^{-1}	
Rate constant (k_{1C})	$1 \cdot 10^{-7}$ ml sec^{-1}	
Recombination (k_{2AC})	$3 \cdot 10^{-6}$ ml sec^{-1}	

if all other parameters in eqn. 23 are kept constant this implies

$$k_1(A)_{max} = \text{constant} \tag{28}$$

Fig. 3 shows a graph of a series of sensitivity calculations using the data in Table I, and only changing the attachment rate constant k_1. The calculation was performed by using literature values for k_p, k_{2e}, k_{2A}, (P^+) and v_e. The value of v'_A was varied so as to best match the experimental roll off in sensitivity for lindane. The value of k_1 was then chosen to yield the same concentration at which the sensitivity was decreased by 10% as was experimentally observed for lindane. The resulting values for v_A and k_1 are physically reasonable, although no literature values are accurately known for these quantities. The detection limits were calculated by assuming a con-

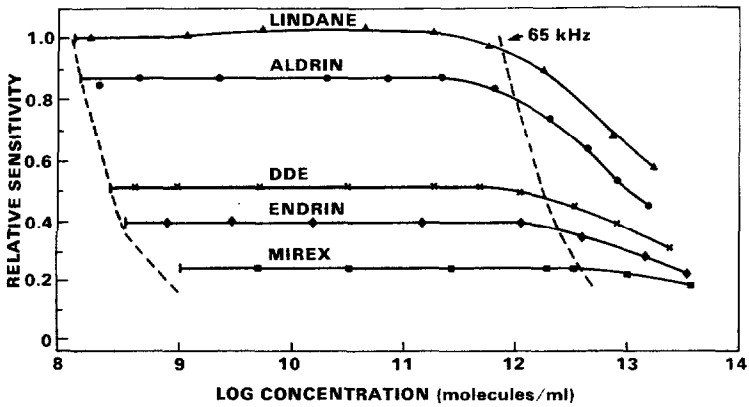

Fig. 2. Experimental sensitivities. Dashed line on right is the interpolated concentration for which the response equals 65 kHz. Reference current $2.96 \cdot 10^{-10}$ A.

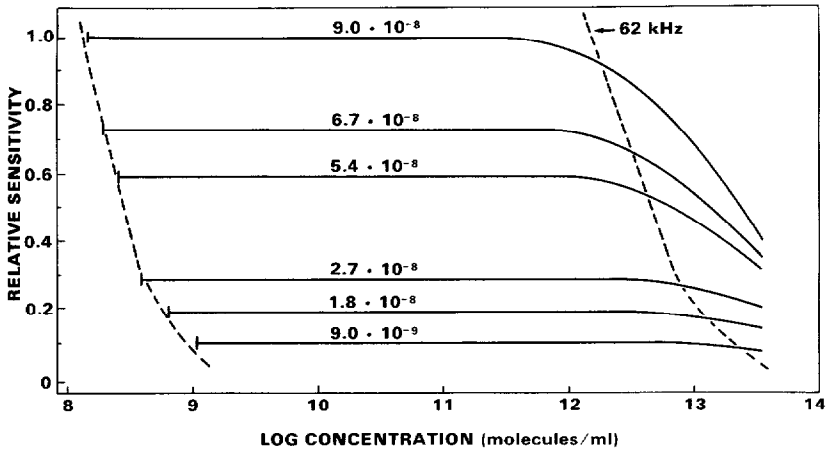

Fig. 3. Calculated sensitivities using the parameters in Table I. Reference current $2.96 \cdot 10^{-10}$ A. Attachment rate constant k_1 is varied from $9 \cdot 10^{-8}$ to $9 \cdot 10^{-9}$ ml sec^{-1}.

stant noise level, due to the presence of an electron-attaching contaminant. Again the calculation confirms that as long as the anions and electron drift velocities remain constant, the pulse frequency at which the sensitivity is decreased by 10%, f_{max}, is always the same even though the concentration C_{max} is different.

The effects of changing the reference current is shown in Fig. 4 using lindane as the test compound. As the reference current I_{ref} is changed, the average electron concentration in the cell changes and therefore the base frequency f_0, and also the frequency at which the non-linear response occurs. However, the sample concentration C_{max} remains the same. The calculated sensitivities shown in Fig. 5 again used the data from Table I and only the reference current was varied. At extremely high concentrations the model predicts a greater loss in sensitivity than is observed. This may be due to the build-up of enough space charge due to the anions, that a counter field has developed[17,18].

As discussed previously the noise level was assumed to be due to the presence

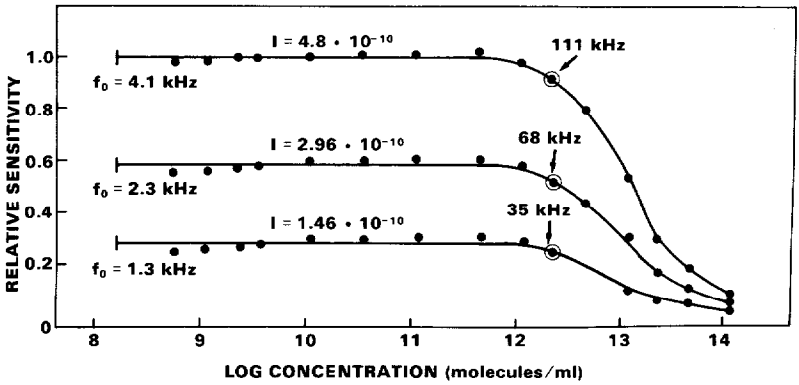

Fig. 4. Experimental sensitivities for lindane. Reference current varied: $1.46 \cdot 10^{-10}$, $2.96 \cdot 10^{-10}$, $4.8 \cdot 10^{-10}$. The circled points are the frequencies where the sensitivities are reduced by 10%.

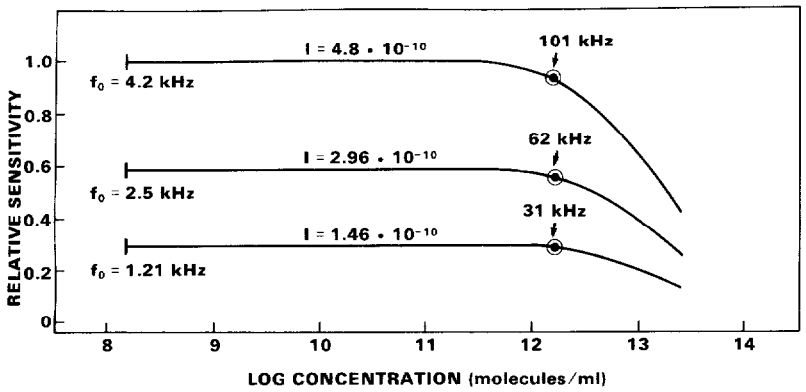

Fig. 5. Calculated sensitivities using the parameters in Table I. Reference current varied: $1.46 \cdot 10^{-10}$, $2.96 \cdot 10^{-10}$, $4.8 \cdot 10^{-10}$. The circled points are the frequencies where the sensitivities are reduced by 10%.

of a contaminant, such as oxygen which is always present at levels of a few ppm. When the reference current is changed, not only is the sensitivity for the sample changed; but also the sensitivity (and the noise level) of the contaminant. Thus the calculations predict that the signal-to-noise ratio will be unchanged. The actual measured signal and noise as a function of base frequency is shown in Fig. 6. The base

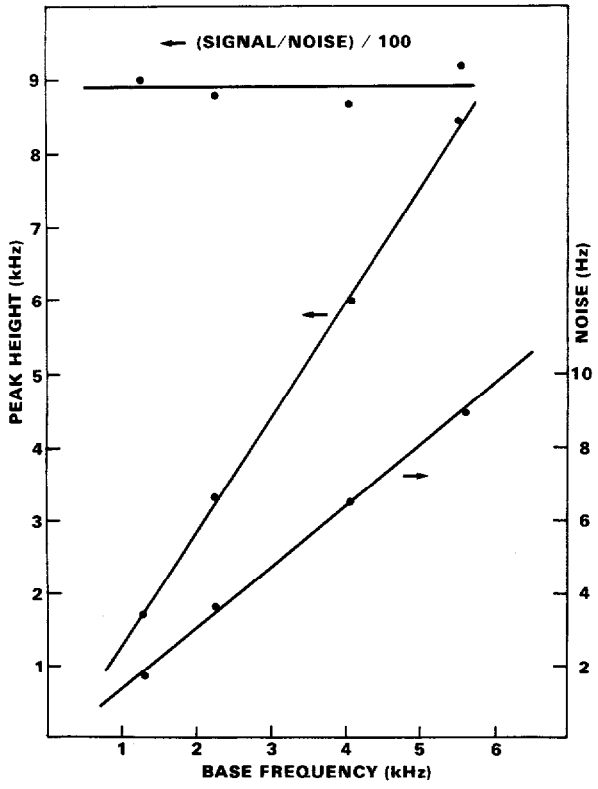

Fig. 6. Experimental response to 16 pg lindane, noise and signal-to-noise ratio.

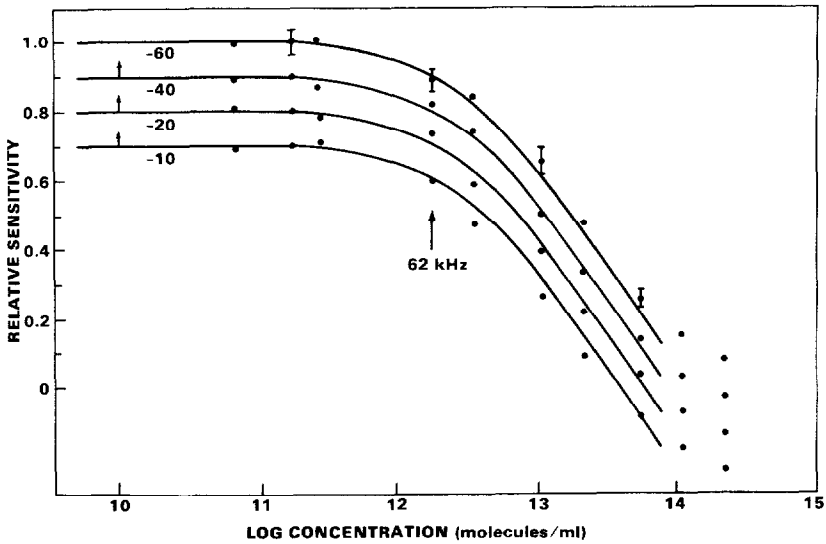

Fig. 7. Experimental sensitivities for lindane for different pulse voltage amplitude: −60, −40, −20 and −10 V. Solid line is calculated as described in text. Curves for −40, −20 and −10 have been displaced down by 0.1, 0.2 and 0.3 units, respectively.

frequency was varied by changing the reference current. It can be seen that the signal-to noise ratio is essentially a constant.

As a final test of the model, the effect of changing the pulse voltage was investigated. As the pulse voltage was changed, the reference current was adjusted so as to have the same base frequency. The experimental points are shown in Fig. 7, along with the calculated (solid) curves. The curves for −40, −20 and −10 V are displaced downward for clarity. The model predicts, and the data confirms within the experimental error, that the response is the same. Each experimental data point is the average of three injections. The experimentally measured reference currents that were required to maintain a constant base frequency were found to vary almost as the square root of the pulse voltage, and are listed in Table II. Also listed are the drift velocities used in the calculation to maintain a constant f_0 when the experimental values of reference current were used. These drift velocities were obtained by iteratively changing them until the same experimental value of f_0 was obtained for each new value of I_{ref}. The value of the anion drift velocity was then changed assuming

TABLE II

CALCULATED DRIFT VELOCITIES
$f_0 = 2.5 \cdot 10^3$ Hz.

U (V) (exp)	I_{ref} ($\cdot 10^{10}$ A) (exp)	v_e (cm/sec) (calc.)	v_A (cm/sec) (calc.)
−60	$3.61 \cdot 10^{-10}$	$3.7 \cdot 10^5$	245
−40	$2.96 \cdot 10^{-10}$	$3.0 \cdot 10^5$	200
−20	$2.14 \cdot 10^{-10}$	$2.2 \cdot 10^5$	146
−10	$1.45 \cdot 10^{-10}$	$1.5 \cdot 10^5$	100

that it changed linearly with the average electric field. The model as presented above predicts a linear relationship between the collected current and the applied potential if all other parameters, including f_0, are kept constant. This is due to the assumption of a uniform electric field within the cell as shown in eqn. 16, which according to eqn. 8 is linearly proportional to the applied voltage. This equation describes the volume of the cell from which electrons can be extracted by the applied field during the time t_p. This volume is given by the product of the cross sectional area of the cell, A, the drift velocity, v_e, and the time interval, t_p. If all other parameters, *i.e.*, f_0, are kept constant, then increasing U will result in a linear increase in the collected current. However, the electric field within the displaced coaxial cell used in this work is not uniform. In a previous paper[15] the electric field distributions for various cell geometries were calculated. It could be seen from the distribution of the equipotential surfaces that the field near the anode in the displaced coaxial cell was similar, although somewhat weaker, than the fields in a coaxial cell of similar dimensions. As a first approximation the coaxial field can be used to estimate the volume of the cell from which charge can be extracted by a given applied potential. The collected current is given by

$$I = \frac{q}{T}(\overline{e^-}) \cdot AR \tag{29}$$

where $(\overline{e^-})$ is the time averaged electron concentration, the last term AR is the volume from which charge can be removed in time t_p, and R is the maximum axial distance from the anode from which an electron can be collected. The latter quantity can be determined from

$$\frac{dr}{dt} = k_e E_r \tag{30}$$

where k_e is the electron mobility[14], r is the axial position of the charge and E_r the electric field intensity for the concentric cylinder symmetry, is given by[19]

$$E_r = \frac{UG}{r} \tag{31}$$

where U is the applied potential and G is a geometry factor.

Integrating eqn. 30 gives

$$\int_0^R \frac{1}{E_r} dr = \int_0^{t_p} K_e dt \tag{32a}$$

$$R = (2UGk_e t_p)^{1/2} \tag{32b}$$

Thus from eqn. 29:

$$I \propto (U)^{1/2} \tag{33}$$

TABLE III

CALCULATED COLLECTION VOLUMES

U (V)	I ($\cdot 10^{10}$ A) (exp)	I^*	V_c^{**}
−60	3.61	2.49	2.15
−40	2.91	2.01	1.80
−20	2.14	1.48	1.35
−10	1.45	1.00	1.00

* Experimental values normalized to I_{ref} at −10 V.

** V_c is the relative collection volume calculated from the electron trajectories.

Therefore the value of the drift velocity used to determine the rate constants in eqn. 8 is not directly proportional to the applied potential, but should represent an average value throughout the region of the cell from which charge can be extracted. This quantity varies more like the square root of the potential.

A more accurate determination of the relation between the applied voltage and the collected current was obtained by numerically calculating the electric field throughout the cell, as was done previously[15] for the voltages listed in Table III. From a uniform distribution of initial points throughout the cell, the equations of motion were solved and the actual trajectories of the electrons were determined. Only those starting points that resulted in a trajectory striking the anode within the time period t_p, were counted in the collection volume. The relative number of points that made up the collection volume at each applied potential, should be proportional to the collected current. The values that were calculated in this manner are listed in Table III and are in reasonable agreement with the experimental values.

In order to prevent the collection of anions at high pulse frequencies a bipolar pulsed circuit has recently been employed[20]. The first pulse was of negative voltage, followed immediately by a positive pulse of equal duration. The results were encouraging. No effect was observed with the bipolar circuit until pulse frequencies greater than 50 kHz were encountered. Beyond this value an increase in linear response was observed as the amplitude of the positive pulse approached that of the negative pulse. An improvement in the linear response by almost an order of magnitude was effected; the improvement being greatest when the base frequency was lowest.

CONCLUSIONS

The model developed in this paper has been shown to be capable of providing a semi-quantitative explanation for the decreased sensitivity of the constant-current electron-capture detector at high sample concentrations. A more accurate calculation requires a more precise determination of the parameters in Table I. In addition is shown that it is not necessary to remove all of the electrons from the cell in order to obtain a linear response. In a future paper additional experimental data will be presented for measured electron and anion contributions in the electron-capture detector, including relative drift velocities obtained under actual electron-capture detection conditions; *i.e.*, atmospheric pressure and high temperature.

It would appear that the continued development of a more accurate model of the electron-capture detector would require a finite element analysis. This approach would allow one to take into account the inhomogeneities of the different processes that are occurring within the cell. The expression given by Grimsrud and Connally[9] would allow the determination of the electron–ion production rate (k_p) at each nodal point within the cell. In a previous paper[15] a numerical solution of Poisson's equation for an arbitrary charge distribution allowed the calculation of electron and anion drift velocities with cells of various geometries. This allows the determination of charge flux (electron, anion and cations) into and out of each nodal point within the cell, due to the applied electric field, *i.e.*, k_{3e} and k_{3A} in eqn. 5 would be known as a function of time and space. The additional field due to the space charge at the surrounding nodal points should now be included. Knowing the charge density at each point would allow the solution of the coupled kinetic eqns. 6 and 7 at each point in space and time without the assumption (P^+) = constant. The integration of these equations with respect to time would determine the collected charge at the anode, for a single pulse cycle. This process would have to be iteratively repeated until a self consistent solution is obtained. The value of being able to solve such a complex model is that it would allow the design of an optimized electron-capture detector from an understanding of all processes that are occurring; not simply those that are the easiest to solve for analytically. The value of simple analytical models such as the one presented in this paper is that it provides a guide for experimental investigations, as well as a check for the more complex numerical simulations.

REFERENCES

1 W. E. Wentworth, E. C. Chen and J. E. Lovelock, *J. Phys. Chem.*, 70 (1966) 445.
2 R. J. Maggs, P. L. Joynes, A. J. Davies and J. E. Lovelock, *Anal. Chem.*, 43 (1971) 1966.
3 I. Śliwka, J. Lasa and J. Rosiek, *J. Chromatogr.*, 172 (1979) 1.
4 P. L. Gobby, E. P. Grimsrud and S. W. Warden, *Anal. Chem.*, 52 (1980) 473.
5 J. E. Lovelock, *J. Chromatogr.*, 99 (1974) 3.
6 J. E. Lovelock and A. J. Watson, *J. Chromatogr.*, 158 (1978) 123.
7 W. B. Knighton and E. P. Grimsrud, *Anal. Chem.*, 55 (1983) 713.
8 W. B. Knighton and E. P. Grimsrud, *J. Chromatogr.*, 288 (1984) 237.
9 E. P. Grimsrud and M. J. Connolly, *J. Chromatogr.*, 239 (1982) 397.
10 M. J. Connolly, W. B. Knighton and E. P. Grimsrud, *J. Chromatogr.*, 265 (1983) 145.
11 E. P. Grimsrud and S. E. Warden, *Anal. Chem.*, 52 (1980) 1842.
12 E. P. Grimsrud, S. H. Kim and P. L. Gobby, *Anal. Chem.*, 51 (1979) 223.
13 J. R. Acton and J. D. Swift, *Cold Cathode Discharge Tubes*, Academic Press, New York, 1963, Ch. 2.
14 E. W. McDanield, *Collosion Phenomena In Ionized Gases*, Wiley, New York, 1964, Ch. 11.
15 G. Wells and R. Simon, *J. High Resolut. Chromatogr. Chromatogr. Commun.*, 6 (1983) 427.
16 G. Wells, *J. High Resolut. Chromatogr. Chromatogr. Commun.*, 6 (1983) 651.
17 W. A. Aue and S. Kapila, *J. Chromatogr.*, 188 (1980) 1.
18 W. A. Aue and K. W. M. Siu, *J. Chromatogr.*, 239 (1982) 127.
19 J. R. Reitz and F. J. Milford, *Foundations of Electromagnetic Theory*, Addison-Wesley, New York, 1967.
20 R. Simon and G. Wells, *J. Chromatogr.*, 302 (1984) 221.
21 T. E. Bortner, G. S. Hurst and W. G. Stone, *Rev. Sci. Instr.*, 28 (1957) 103.
22 G. H. Wannier, *Bell Syst. Tech. J.*, 32 (1953) 170.
23 T. Fujii and G. G. Meisels, *J. Chem. Phys.*, 75 (1981) 5067.
24 J. C. Tou, R. Ramstad and T. J. Nestrick, *Anal. Chem.*, 51 (1979) 781.
25 G. Wells, *J. Chromatogr.*, 285 (1984) 395.
26 L. G. Christophorou, *Chem. Rev.*, 76 (1976) 409.